JACS
JOURNAL OF THE AMERICAN CHEMICAL SOCIETY

ARTICLE

pubs.acs.org/JACS

Turnover Is Rate-Limited by Deglycosylation for *Micromonospora viridifaciens* Sialidase-Catalyzed Hydrolyses: Conformational Implications for the Michaelis Complex

Jefferson Chan, April Lu, and Andrew J. Bennet*

Departments of Chemistry and Molecular Biology and Biochemistry, Simon Fraser University, 8888 University Drive, Burnaby, British Columbia V5A 1S6, Canada

Supporting Information

ABSTRACT: A panel of seven isotopically substituted sialoside natural substrate analogues based on the core structure 7-(5-acetamido-3,5-dideoxy-D-*glycero*-α-D-*galacto*-non-2-ulopyranosylonic acid)-(2→6)-*β*-D-galactopyranosyloxy)-8-fluoro-4-methylcoumarin (**1**, Neu5Acα2,6Gal*β*FMU) have been synthesized and used to probe the rate-limiting step for turnover by the *M. viridifaciens* sialidase. The derived kinetic isotope effects (KIEs) on k_{cat} for the ring oxygen (^{18}V), leaving group oxygen (^{18}V), anomeric carbon (^{13}V), C3-carbon (^{13}V), C3-*R* deuterium ($^{D}V_R$), C3-*S* deuterium ($^{D}V_S$), and C3-dideuterium ($^{D}_2V$) are 0.986 ± 0.003, 1.003 ± 0.005, 1.021 ± 0.006, 1.001 ± 0.008, 1.029 ± 0.007, 0.891 ± 0.008, and 0.890 ± 0.006, respectively. The solvent deuterium KIE (^{D_2O}V) for the sialidase-catalyzed hydrolysis of **1** is 1.585 ± 0.004. In addition, a linear proton inventory was measured for the rate of hydrolysis, under saturating condition, as a function of *n*, the fraction of deuterium in the solvent. These KIEs are compatible with rate-determining cleavage of the enzymatic tyrosinyl *β*-sialoside intermediate. Moreover, the secondary deuterium KIEs are consistent with the accumulating Michaelis complex in which the sialosyl ring of the carbohydrate substrate is in a $^{6}S_2$ skew boat conformation. These KIE measurements are also consistent with the rate-determining deglycosylation reaction occurring via an exploded transition state in which synchronous charge delocalization is occurring onto the ring oxygen atom. Finally, the proton inventory and the magnitude of the solvent KIE are consistent with deglycosylation involving general acid-catalyzed protonation of the departing tyrosine residue rather than general base-assisted attack of the nucleophilic water.

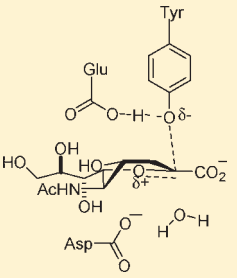

INTRODUCTION

exo-Sialidases (neuraminidases; EC 3.2.1.18) are a class of glycosyl hydrolases (GH) that catalyze the hydrolysis of the α-ketosidic bond linking terminal sialic acid residues to various glycoconjugates. These enzymes have been identified to play important roles in a number of human pathologies, including cancer,[1,2] cholera,[3] and influenza.[4] All *exo*-sialidases, characterized to date, are retaining glycosidases in which a double inversion of configuration occurs so that the first released product has the same anomeric stereochemistry as that of the substrate.[5] It has been established through mutagenesis[6−9] and fluoro-sugar labeling studies[10,11] that an active-site tyrosine residue acts as a nucleophile during the catalytic cycle to generate a covalently linked *β*-sialosyl-enzyme intermediate. This glycosylation step has been proposed to proceed via either concerted S_N2 (A_ND_N)[12] or stepwise S_N1 ($D_N + A_N$)[13] pathways. Subsequent hydrolysis of the enzyme bound intermediate followed by product release completes the catalytic cycle. The sialidase from the soil bacterium *Micromonospora viridifaciens* displays a very high catalytic efficiency ($k_{cat}/K_m > 10^7$ M^{-1} s^{-1}, for activated substrates),[6,14] broad substrate specificity,[14] and a remarkable tolerance to mutation of its active site residues.[6−9] The mechanism for sialidase-catalyzed hydrolysis has been probed by Brønsted analyses,[15] where the derived β_{lg} values have provided valuable information regarding the identity of rate-determining steps.[6,16−18] Specifically, negative β_{lg} values suggest that glycosylation is at least partially rate-limiting for the appropriate kinetic term, as is the case with *Vibrio cholerae* sialidase ($\beta_{lg}(V/K) = -0.73$; $\beta_{lg}(V) = -0.25$).[17] The β_{lg} values on V/K and V for *Micromonospora viridifaciens* sialidase-catalyzed hydrolyses were reported to be −0.30 + 0.04 and 0.02 + 0.03, respectively.[6] Together, these results suggest that glycosidic bond cleavage is at least partially rate-limiting for k_{cat}/K_m, but that k_{cat} is limited by a subsequent step. In other words, the possible rate-determining steps for enzymatic turnover (k_{cat}) are: (i) deglycosylation of the sialosyl-enzyme intermediate; (ii) a conformational change of the initial bound α-sialic acid:enzyme product complex; or (iii) product release. Given that only deglycosylation, of the possible rate-limiting steps, involves covalent bond formation and cleavage, it is likely that kinetic isotope effects (KIEs) on V will allow a distinction to be made between these three possibilities.

The current study expands upon a previously established coupled-enzyme assay using natural sialoside analogues, which was used to determine enzymatic rate constants,[19] for the measurement of a series of secondary deuterium and heavy-atom

Received: October 13, 2010
Published: February 15, 2011

dx.doi.org/10.1021/ja109199p | *J. Am. Chem. Soc.* 2011, 133, 2989–2997

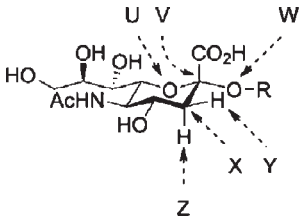

1a. V = ^{13}C
1b. U = ^{18}O
1c. X = ^{13}C
1d. W = ^{18}O
1e. Z = ^{2}H
1f. Y = ^{2}H
1g. Z = Y = ^{2}H

Figure 1. Isotopically labeled compounds used in the measurement of KIEs on k_{cat} for *M. viridifaciens* sialidase-catalyzed hydrolysis of the natural substrate analogue Neu5Acα2,6Galβ*F*MU.

KIEs using a panel of seven isotopically labeled substrates (Figure 1).

■ MATERIALS AND METHODS

Materials. Cytidine 5′-triphosphate disodium salt was purchased from 3B Scientific Corp. All other reagents were purchased from Aldrich and used without purification. Thin-layer chromatography (TLC) was performed on aluminum-backed TLC plates precoated with Merck silica gel 60 F254. Compounds were visualized with UV light and/or staining with a *p*-anisaldehyde solution. Flash chromatography was performed using silica gel 60 (230−400 mesh). Solvents used for anhydrous reactions were dried and distilled immediately prior to use. THF was dried and distilled over sodium metal, and dichloromethane was dried and distilled over calcium hydride. For anhydrous reactions, all glassware was flame-dried and cooled under a nitrogen atmosphere immediately prior to use. NMR spectra were recorded on a Bruker 600 MHz spectrometer. Chemical shifts (δ) are listed in ppm downfield from TMS. All NMR peak assignments are based on ^{1}H−^{1}H COSY and ^{1}H−^{13}C HMQC experiments; coupling constants are reported in Hz. *E. coli* sialic acid (Neu5Ac) aldolase was purchased from Codexis. *Neisseria meningitidis*, CMP-NeuAc synthase, was expressed and purified as reported,[20] and the α-2,6-sialyltransferase from *Photobacterium* sp. JT-ISH-224 was kindly donated by M. Gilbert (National Research Council, Ottawa). *A. oryzae* β-galactosidase was purchased from Sigma-Aldrich. *M. viridifaciens* sialidase was expressed recombinantly in *E. coli* and purified as described.[6] The ^{13}C-labeled sodium pyruvates (99.9 atom %) were purchased from Cambridge Isotopes, and ^{18}O-labeled H_2O was purchased from Marshall isotopes (95.1 atom % O-18, batch no. 020414nw). Labeled C3-deuterated Neu5Ac[21] and 2-acetamido-2-deoxy-D-(3-^{18}O)mannose[22] were synthesized as reported in the literature. The synthesis of 8-fluoro-4-methylumbellyferyl β-galactopyranoside, which upon β-galactosidase-catalyzed hydrolysis gives the fluorescent 8-fluoro-7-hydroxy-4-methylcoumarin (8-fluoro-4-methylumbellyfereone, FMU), is given in the Supporting Information. In addition, the Supporting Information contains the ^{1}H NMR spectra of **1** and all of its labeled isotopomers, the ^{13}C NMR spectra of **1** and the two ^{13}C-labeled substrates, and the HR−MS *m*/*z* data for all isotopomers.

Synthesis of (6-^{18}O)Galactoside Precursor. Preparation of compound **1b** requires synthesis of 8-fluoro-4-methylumbellyferyl β-D-(6-^{18}O)galactopyranoside ^{18}O-**6**, which can be accessed in six steps beginning from D-galactose in 8.0% yield overall as detailed below.

*1,2:3,4-Di-O-isopropylidene-α-D-galactopyranose (**2**).* A suspension of D-galactose (4.9 g, 27.2 mmol) in acetone (100 mL) was treated with $ZnCl_2$ (3.70 g, 27.2 mmol) and concentrated H_2SO_4 (0.1 mL). The resultant mixture was stirred at room temperature for 20 h. Potassium carbonate (1.0 g) was added, and the resultant mixture was stirred for 10 min. The reaction mixture was filtered through a Celite plug and washed with acetone. The filtrate and washings were concentrated under reduced pressure to afford the desired product as a colorless syrup (6.95 g, 26.7 mmol, 98% yield). ^{1}H NMR (600 MHz, $CDCl_3$): δ 5.60 (d, *J* = 5.0, 1H, H-1), 4.64 (dd, *J* = 7.9, 2.4, 1H, H-3), 4.37 (dd, *J* = 5.0, 2.4, 1H, H-2), 4.30 (dd, *J* = 7.9, 1.6, 1H, H-4), 3.95−3.86 (m, 2H, H-5, H-6), 3.78 (dd, *J* = 15.7, 7.8, 1H, H-6′), 2.13 (bs, 1H, OH), 1.56 (s, 3H, CH_3), 1.49 (s, 3H, CH_3), 1.37 (s, 6H, 2 × CH_3). ^{13}C NMR (151 MHz, $CDCl_3$): δ 109.01, 108.21, 95.84, 71.18, 70.30, 70.11, 67.57, 61.94, 25.57, 25.46, 24.47, 23.83. Anal. Calcd for $C_{12}H_{20}FO_6$: C, 55.37; H, 7.74. Found: C, 55.17; H, 7.81.

*6-O-(18O)-Benzoyl-1,2:3,4-di-O-isopropylidene-α-D-(6-18O)galactopyranose (**3**).* A flame-dried flask was charged with **2** (500 mg, 1.92 mmol), ($^{18}O_2$)-benzoic acid (300 mg, 2.38 mmol),[12] PPh_3 (655 mg, 2.49 mmol), and anhydrous THF (25 mL). The reaction mixture was cooled in an ice bath and treated with a 40% solution of diethyl azodicarboxylate in toluene (1.1 mL, 2.3 mmol). After being stirred at room temperature overnight, the solvent was removed under reduced pressure, and the resultant residue was purified via flash chromatography (3:17 v/v EtOAc/hexanes) to afford the desired product as a syrup (371 mg, 0.96 mmol, 50.0%). ^{1}H NMR (600 MHz, $CDCl_3$): δ 8.13−8.04 (m, 2H, Ar−H), 7.63−7.54 (m, 1H, Ar−H), 7.51−7.42 (m, 2H, Ar−H), 5.60 (d, *J* = 5.0, 1H, H-1), 4.68 (dd, *J* = 7.9, 2.5, 1H, H-3), 4.56 (dd, *J* = 11.5, 4.9, 1H), 4.46 (dd, *J* = 11.5, 7.6, 1H), 4.40−4.34 (m, 2H, H-2), 4.26−4.17 (m, 1H, H-5), 1.55 (s, 3H, CH_3), 1.50 (s, 3H, CH_3), 1.39 (s, 3H, CH_3), 1.36 (s, 3H, CH_3). ^{13}C NMR (151 MHz, $CDCl_3$): δ 165.92, 132.51, 129.60, 129.24, 127.87, 109.23, 108.35, 95.87, 70.68, 70.27, 70.08, 65.68, 63.37, 25.55, 25.51, 24.51, 24.03.

*1,2,3,4-Tetra-O-acetyl-6-O-(18O)benzoyl-D-(6-18O)galactopyranose (**4**).* A solution of **3** (300 mg, 0.82 mmol) in 80% aqueous AcOH (10 mL) was stirred at 75 °C for 30 min. The solvent was evaporated under reduced pressure to yield a syrup that was then treated with a 2:1 mixture of pyridine:Ac_2O (20 mL) and stirred overnight at room temperature. The reaction mixture was diluted with CH_2Cl_2 (50 mL) and washed successively with water (50 mL), 10% H_2SO_4 (50 mL), saturated $NaHCO_3$ (mL), and brine (50 mL). The organic layer was dried (Na_2SO_4) and concentrated. The resultant residue was purified via flash chromatography (1:1 v/v EtOAc/hexanes) to afford the desired product as a colorless syrup (357 mg, 0.7 mmol, 80%). ^{1}H NMR (600 MHz, $CDCl_3$): δ 8.05−7.98 (m, 2H, Ar−H), 7.63−7.57 (m, 1H, Ar−H), 7.50−7.44 (m, 2H, Ar−H), 6.44 (d, *J* = 3.1, 1H, H-1), 5.67−5.62 (m, 1H, H-3), 5.41 (dd, *J* = 5.2, 3.0, 2H, H-2, H-4/H-5), 4.53−4.44 (m, 2H, H-4/H-5, H-6), 4.30 (dd, *J* = 10.9, 6.9, 1H, H-6), 2.21 (s, 3H, CH_3), 2.19 (s, 3H, CH_3), 2.05 (d, *J* = 3.9, 3H, CH_3), 2.03 (d, *J* = 3.9, 3H, CH_3). ^{13}C NMR (151 MHz, $CDCl_3$): δ 169.63, 169.61, 169.43, 168.47, 165.40, 132.90, 129.31, 129.27, 128.80, 128.03, 89.29, 68.34, 67.06, 66.88, 66.04, 60.99, 20.42, 20.18, 20.16, 20.08.

*8-Fluoro-4-methylumbelliferyl 2,3,4-Tri-O-acetyl-6-O-(18O)benzoyl-β-D-(6-18O)galacto-pyranoside (**5**).* A solution of 33% HBr in AcOH (60 mL) and Ac_2O (11 mL) was cooled to 0 °C in an ice bath and treated with **4** (3.09 g, 6.8 mmol). After being warmed and stirred at room temperature for 2 h, the reaction mixture was diluted with CH_2Cl_2 (150 mL) and poured into ice−water (∼100 mL). After separation of the organic phase, it was washed with saturated $NaHCO_3$ (150 mL), dried (Na_2SO_4), and concentrated. The resultant residue was treated with 8-fluoro-4-methylumbelliferone (1.31 g, 6.8 mmol), tetrabutylammonium bromide (1.95 g, 6.0 mmol), CH_2Cl_2 (285 mL), and 0.67 M aqueous NaOH (38 mL, 25.4 mmol). After being stirred for 1.5 h, the reaction was quenched by the addition of saturated NH_4Cl (20 mL), and the resulting solution was extracted with EtOAc (3 × 100 mL). The organic fractions were dried (Na_2SO_4) and concentrated. The residue was purified by flash chromatography (1:39 v/v MeOH:CH_2Cl_2) to afford the desired product as a white solid (1.10 g, 1.9 mmol, 27.6% over two steps). mp = 88−89 °C. ^{1}H NMR (600 MHz, $CDCl_3$): δ 8.08−8.00 (m, 2H, Ar−H), 7.66−7.59 (m, 1H, Ar−H), 7.54−7.43 (m, 2H, Ar−H), 7.16−7.03 (m, 2H, Ar−H), 6.26 (d, *J* = 1.2, 1H, Ar−H), 5.63−5.55 (m, 2H), 5.23−5.15 (m, 1H), 5.09 (d, *J* = 7.9, 1H), 4.61 (dd, *J* = 11.4, 7.5, 1H), 4.38 (dd, *J* = 11.4, 5.8, 1H), 4.25−4.18 (m, 1H), 2.38 (s, 3H, CH_3), 2.25 (s, 3H, CH_3), 2.14 (s, 3H, CH_3), 2.06 (s, 3H, CH_3). ^{13}C NMR (151

Scheme 1. One-Pot Three-Enzyme Chemoenzymatic Synthesis of Neu5Acα2,6Galβ*FMU*

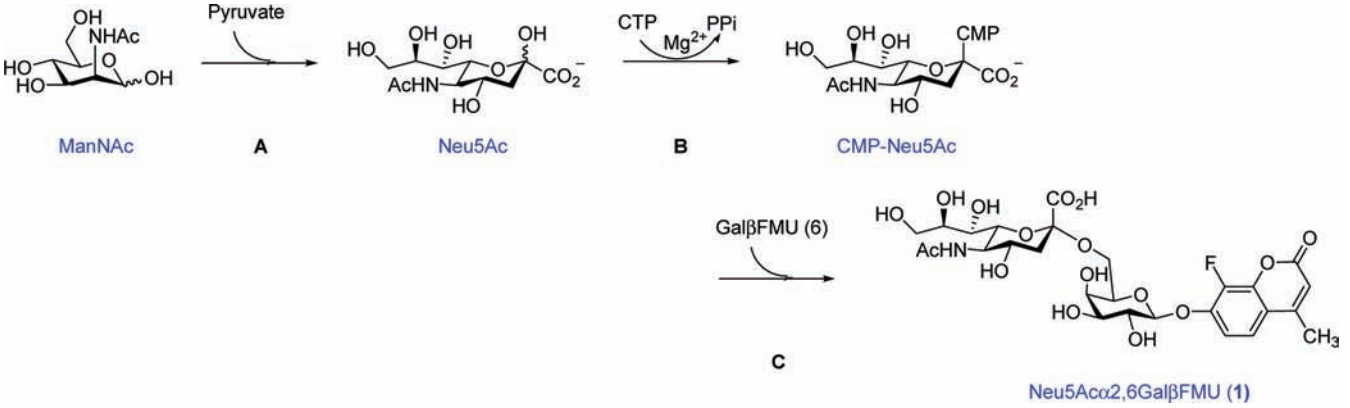

MHz, $CDCl_3$): δ 169.69, 169.58, 168.98, 165.32, 158.66, 151.27, 146.32, 146.26, 142.59, 141.33, 139.65, 132.98, 129.31, 128.83, 128.05, 118.53, 118.50, 116.90, 114.71, 113.76, 100.66, 71.14, 70.08, 67.93, 66.41, 61.22, 20.21, 20.16, 20.10, 18.25.

*8-Fluoro-4-methylumbelliferyl β-D-(6-^{18}O)Galactopyranoside (^{18}O-**6**).* A solution of **5** (100 mg, 0.169 mmol) in 0.5 M NaOMe in MeOH (20 mL) was stirred at room temperature for 1.5 h. After 30 min, a white solid began to precipitate. The precipitate was collected via filtration and rinsed with Et_2O. Upon drying, the desired product was obtained as a white solid (45 mg, 0.126 mmol, 74.3%). mp = 181−182 °C. ^{1}H NMR (600 MHz, DMSO): δ 7.55 (dd, *J* = 9.1, 1.5, 1H, Ar−H), 7.30 (dd, *J* = 9.0, 7.5, 1H, Ar−H), 6.35 (d, *J* = 1.2, 1H, Ar−H), 5.34 (bs, 1H, OH), 5.10 (d, *J* = 7.7, 1H, H-1), 4.94 (bd, *J* = 4.5, 1H, OH), 4.67 (bs, 1H, OH), 4.59 (bs, 1H, OH), 3.73 (s, 1H), 3.70−3.60 (m, 2H), 3.60−3.51 (m, 1H), 3.51−3.40 (m, 2H), 2.43 (s, *J* = 1.1, 3H, CH_3). ^{13}C NMR (151 MHz, DMSO): δ 158.77, 153.38, 147.48, 147.43, 142.21, 142.15, 139.62, 137.98, 120.35, 115.03, 112.37, 112.11, 100.91, 75.80, 73.26, 70.02, 68.02, 60.22, 18.19. Anal. Calcd for $C_{16}H_{17}FO_7{}^{18}O_1$: C, 53.63; H, 4.78. Found: C, 53.37; H, 4.81.

Synthesis and Purification of Neu5Acα2,6Galβ*FMU*. A 50 mL autoclaved falcon tube was charged with *N*-acetyl-D-mannosamine (50.0 mg, 226 μmol), sodium pyruvate (37.3 mg, 339 μmol), H_2O (2.5 mL), and *E. coli* Neu5Ac aldolase (2 mg). The reaction vessel was incubated and shaken at 37 °C for 3 h. Subsequently, cytidine 5′-triphosphate disodium salt (178.7 mg, 339 μmol), 1.0 M tris (2.5 mL), 1.0 M $MgCl_2$ (1.0 mL), 1.0 M dithiothreitol (1.5 μL), and CMP-Neu5Ac synthase (0.6 mL, 50 U/mL) were added to the reaction mixture. After a further incubation at 37 °C for approximately 1.5 h, the reaction mixture was centrifuged (10 min @ 2500 rpm). The supernatant was separated from the pellet and transferred to a new 50 mL autoclaved falcon tube, after which Galβ*FMU* (**6**, 50.1 mg, 103 μmol) and α2,6-sialyl transferase (0.5 mL, 2.1 U/mL) were added to the solution, and the resultant mixture was incubated at 37 °C overnight. The reaction mixture was loaded onto a reversed-phased C18 sep-pak cartridge (20 cc, 5 g), and the cartridge was eluted successively with H_2O (∼50 mL) and 1:19 v/v MeCN/H_2O (∼150 mL). The fractions containing product were pooled and lyophilized to afford the product as a white solid. Typical yields ranged from 35% to 40%. Samples of Neu5Acα2,6Galβ*FMU* in H_2O were then loaded onto a HP/Agilent 1100 equipped with a C6 reverse phase HPLC column equilibrated in 95% solvent A (0.1% TFA in H_2O) and 5% solvent B (100% MeCN-0.1% TFA). The desired analytically pure substrate was eluted from the column by increasing the gradient of solvent B over 30 min from 5% to 30%. The column flow rate was maintained at 2 mL/min, and 300 μL fractions were collected. The absorbance of the effluent was monitored at 340 nm. All labeled Neu5Acα2,6Galβ*FMU* exhibited the predicted ^{1}H and ^{13}C NMR spectra consistent with incorporation of isotopes (^{2}H, ^{13}C, and ^{18}O) at the expected positions. Unlabeled Neu5Acα2,6Galβ*FMU*, ^{1}H NMR (600 MHz, D_2O): δ 7.53 (d, *J* = 9.1, 1H, Ar−H), 7.25 (dd, *J* = 8.9, 7.5, 1H, Ar−H), 6.26 (d, *J* = 0.9, 1H, Ar−H), 5.10 (s, 1H, 1-H), 3.93−3.85 (m, 3H, 4-H, 5′-H), 3.80 (m, 1H, 2-H), 3.74−3.70 (m, 3H, 3-H), 3.65−3.54 (m, 4H, 4′-H), 3.51 (m, 1H), 3.44 (m, 1H), 2.70−2.61 (m, 1H, 3′-H_{eq}), 2.40 (s, 3H, Ar−CH_3), 1.91 (s, 3H, CH_3), 1.55 (t, *J* = 12.1, 1H, 3′-H_{ax}). ^{13}C NMR (151 MHz, D_2O): 174.96 (C═O, amide), 173.51 (C-1″), 162.46 (Ar), 155.52 (Ar), 146.37 (d, J_{CF} = 8.1 Hz, C-10), 141.48 (d, J_{CF} = 8.8 Hz, C-7), 140.31 (Ar), 139.00 (d, J_{CF} = 248.2 Hz, C-8), 119.19 (d, J_{CF} = 4.1 Hz, C-6), 116.00, 112.41, 111.57, 100.78 (C-1′), 99.04 (C-2″), 74.09 (C-4′), 72.31 (C-2′), 71.68, 70.27, 68.35, 68.13, 67.76, 62.98, 62.55 (C-5″), 51.79 (C-4″), 40.19 (C-3″), 21.93 (CH_3, FMU), 18.05 (CH_3). HR−MS *m*/*z* (M + H^+), $C_{27}H_{34}FNO_{16}$ requires 648.1934, found 648.1929.

Enzyme Kinetics. Michaelis−Menten kinetic parameters for *M. viridifaciens* sialidase and *A. oryzae* β-galactosidase were determined from a minimum of seven initial rate measurements within a substrate concentration range of at least K_m/4 to 4K_m at 25 °C. The progress of the reactions was continuously monitored for 5 min using a Cary Eclipse fluorescence spectrometer equipped with a temperature controller. Each 500 μL reaction mixture was prepared by addition of the appropriate volume of buffer, substrate, and enzyme. The rate versus substrate data were fitted to the Michaelis−Menten equation using a standard nonlinear least-squares program Prism 4.0.

Test for Possible Product Inhibition. Employing conditions identical to those used during the coupled-enzyme assays, the initial rate for 4-methylumbelliferyl *N*-acetyl-α-D-neuraminic acid (MU-NANA) hydrolysis was determined in the presence of varying concentrations of FMU, Neu5Ac, and galactose.

KIE Measurements. The stability of the enzyme solution (containing 0.1 mg/mL BSA), incubated at 25 °C, was evaluated by testing sialidase activity with the substrate MU-NANA at periodic intervals. The measured enzyme activity remained invariant within experimental error for over 48 h. Measurements of KIEs were performed at 25 °C in 100 mM MES ([BSA] = 0.1 mg/mL), adjusted to pH = 5.85. Concentrations of least 7 times the K_m value of **1** were used. The fraction of substrate hydrolyzed during the course of the KIE measurements did not exceed 5%. The analysis order of the isotopically labeled compounds was alternated (i.e., ^{1}H ^{2}H ^{2}H ^{1}H ^{1}H ^{2}H ^{2}H ^{1}H ^{1}H ^{2}H, etc.). Consecutive pairs of kinetic runs were compared, and the mean and standard deviation of at least seven such dyads were taken. A double-blind procedure was used whereby the identities of the "labeled" and "unlabeled" samples used in the experiments were unknown to both

dx.doi.org/10.1021/ja109199p | *J. Am. Chem. Soc.* 2011, 133, 2989–2997

Scheme 2. Preparation of (6-^{18}O)Galactoside Precursor ^{18}O-6

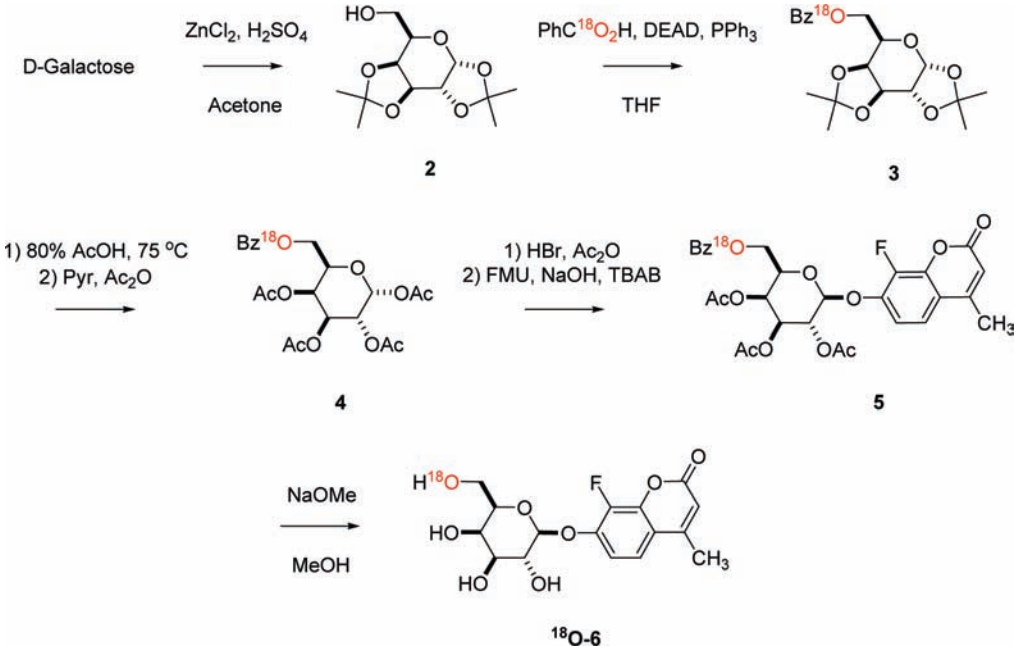

Scheme 3. Coupled Enzyme Assay for the Continuous Measurement of Sialidase Activity

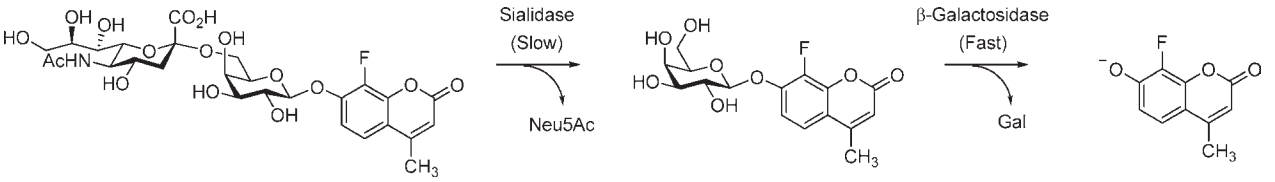

experimenters. Specifically, samples marked as "A" and "B" were prepared by experimenter 1, and the relative concentrations were adjusted to <1% difference based on UV−vis absorbance by experimenter 2, who then relabeled the samples "C" and "D".

Solvent Kinetic Isotope Effect. Buffers were prepared by adding equivalent amounts of NaOH or NaOD to MES in H_2O or D_2O, respectively. Reaction rates were determined at varying deuterium fractions by mixing the H_2O and D_2O buffers accordingly. Substrate concentrations ($7 \times K_m$) in H_2O and D_2O buffers were adjusted to <1% difference based on the UV−vis spectra of each stock solution. To ensure that the enzyme concentrations do not impact the observed rates, the same enzyme stock solution in H_2O was added into each reaction. After dilution, the total H_2O content from the enzyme solution was less than 2% of the total volume.

RESULTS

Substrate Synthesis. Neu5Acα2,6GalβFMU (**1**) and the necessary seven labeled isotopologues (**1a**−**g**) were prepared chemoenzymatically from the β-D-galactopyranoside precursor **6**, ManNAc, and pyruvate (Scheme 1). The labeled starting materials for the seven isotopically substituted substrates were (i) pyruvate (**1a** and **1c**); (ii) deuterated sialic acid (**1e**, **1f**, and **1g**);[21] (iii) *N*-acetyl-3-^{18}O-mannosamine (**1b**);[22] and (iv) ^{18}O-**6**, the synthesis of which is shown in Scheme 2 (**1d**). Enzyme-mediated synthesis of **1** was used for the current study because, in contrast to most chemical syntheses, formation of the glycal 5-acetamido-2,6-anhydro-3,5-dideoxy-D-*glycero*-D-*galacto*-non-2-enonic acid (Neu2en5Ac), a potent inhibitor of sialidases, does not occur during the enzymatic coupling reaction.

Test for Possible Product Inhibition. To ensure that the products released during the kinetic assays did not affect the measured rate of reaction by lowering the sialidase activity, the products of hydrolysis were screened for possible product inhibition. No inhibition was observed up to at least 25 μM FMU, 680 μM Neu5Ac, and 650 μM galactose.

Enzyme Kinetics. To measure KIEs on *V* with natural substrate analogues, it is necessary to ensure that the coupled-enzyme assay reports on the rate of the sialidase-catalyzed reaction (Scheme 3).

Thus, it was checked that doubling the concentration of *A. oryzae* β-galactosidase did not change the observed rate. Furthermore, at constant β-galactosidase concentrations, halving or doubling the concentration of *M. viridifaciens* sialidase results in a corresponding change of the observed rate. The fluorescence intensity of the galactoside aglycone (FMU) was found to be linear up to concentrations of at least 25 μM. This concentration corresponds to ~5% hydrolysis. No photobleaching of FMU was observed under the experimental conditions over a time-course of 60 min. KIE experiments were performed at substrate

dx.doi.org/10.1021/ja109199p | *J. Am. Chem. Soc.* 2011, 133, 2989–2997

Table 1. Kinetic Isotope Effects on k_{cat} for the *M. viridifaciens* Sialidase-Catalyzed Hydrolysis of 1 in 100 mM MES Buffer pH = 5.85, [BSA] = 0.1 mg/mL, and Temperature = 25 °C

compound	site of substitution	KIE[a]	weighted average[b]
1a	anomeric 2-^{13}C	1.022 ± 0.008	1.021 ± 0.006
		1.020 ± 0.008	
1b	ring oxygen 6-^{18}O	0.986 ± 0.004	0.986 ± 0.003
		0.984 ± 0.006	
		0.989 ± 0.010	
1c	C3-^{13}C	1.002 ± 0.010	1.001 ± 0.008
		1.001 ± 0.012	
1d	leaving group 2-^{18}O	1.003 ± 0.006	1.003 ± 0.005
		1.002 ± 0.010	
		1.003 ± 0.011	
1e	axial (3*R*)-^{2}H	1.035 ± 0.012	1.029 ± 0.007
		1.027 ± 0.011	
		1.025 ± 0.018	
1f	equatorial (3*S*)-^{2}H	0.890 ± 0.012	0.891 ± 0.008
		0.893 ± 0.014	
		0.890 ± 0.014	
1g	dideutero 3-^{2}H$_2$	0.885 ± 0.014	0.890 ± 0.006
		0.897 ± 0.009	
		0.885 ± 0.011	
		0.881 ± 0.009[c]	
control	n/a	1.002 ± 0.008[d]	n/a

[a] Average and standard error from at least seven dyad measurements. [b] Calculated according to ref 47. [c] Concentration of **1** was doubled (~14 × K_m), n = 3. [d] Control experiment represents a ratio of observed rates between two separately prepared batches of unlabeled **1**, n = 5.

concentrations of at least 7 times the K_m value of **1**. Listed in Table 1 are averaged KIE values from the last seven consecutive dyad measurements that are corrected to account for incomplete isotopic substitution according to either a literature procedure[23] or, for the case of the β-secondary deuterium effects where unlabeled, monodeuterated, and dideuterated isotopomers are present, eq 1 where f_{HH}, f_{HD}, f_{DH}, and f_{DD} are the fractions of each isotopomer present in the sample. For the dideuterio isotopomer (**1g**), the deuteration at C3 was assumed to be complete (i.e., f_{DD} = 1 and f_{HH} = f_{HD} = f_{DH} = 0).

$$KIE_{obs} = \frac{k_{HH}}{(f_{HH} \times k_{HH}) + (f_{HD} \times k_{HD}) + (f_{DH} \times k_{DH}) + (f_{DD} \times k_{DD})} \quad (1)$$

Solvent Isotope Effects. The solvent deuterium KIE (^{D_2O}V) for the sialidase-catalyzed hydrolysis of **1** was measured to be 1.585 ± 0.004. A proton inventory for this reaction displayed a linearly correlation between the rate of hydrolysis and n, the fraction of deuterium in the solvent (Figure 2).

DISCUSSION

Mechanism of Sialidase-Catalyzed Reactions. The prevailing mechanism for *exo*-sialidases is shown in Scheme 4,[16] where αNeu5Ac−OR is the substrate, αNeu5Ac−OH is the sialic acid product, and the pyranosyl conformations chair and boat are indicated by the subscripts C and B, respectively. For sialidase reactions that are followed under initial rate conditions, the first irreversible event is glycosylation to give the tyrosinyl-enzyme bound intermediate (k_5, Scheme 4).

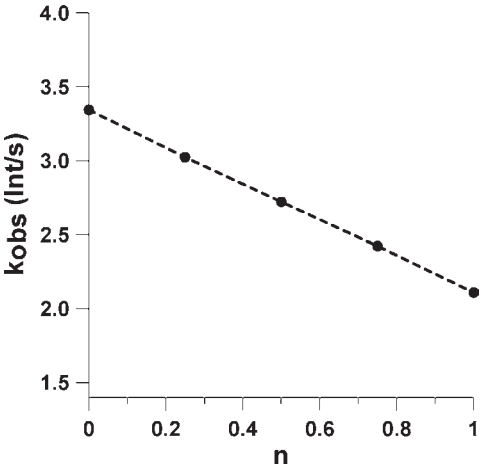

Figure 2. Variation of observed rate constant for *M. viridifaciens* sialidase-catalyzed hydrolysis at saturating concentrations of Neu5Acα2,6Galβ*F*MU in mixtures of H_2O:D_2O; n is the fraction of deuterium in the mixture.

$$\frac{k_{cat}}{K_m} = \frac{k_1 k_3 k_5}{k_2(k_4 + k_5) + k_3 k_5} \quad (2)$$

$$k_{cat} = \frac{k_g k_{dc}}{k_g + k_{dc}} \quad (3)$$

$$k_g = \frac{k_3 k_5}{k_3 + k_4 + k_5} \quad (4)$$

$$k_{dc} = \frac{k_7 k_9 k_{11}}{k_7(k_9 + k_{10} + k_{11}) + k_9 k_{11}} \quad (5)$$

The observed rate constants that are obtained from the Michaelis−Menten parameters for the mechanism shown in Scheme 2 are given by eqs 2 and 3, where k_g (glycosylation) and k_{dc} (deglycosylation, conformational change and product release) are given by eqs 4 and 5, respectively.

The sialidase from *M. viridifaciens* has been shown to exhibit β_{lg} values for hydrolysis on V/K and V of −0.30 ± 0.04 and 0.02 ± 0.03, respectively.[6] These observations require that a step following glycosylation is rate-determining for V.[6] Product release can be ruled out as the rate-determining step on V for the *M. viridifaciens* sialidase because this would require that product inhibition be observed during catalysis. However, little or no inhibition of catalysis is observed at sialic acid concentrations of up to 680 μM. Thus, it can be concluded that k_{11} is much greater than either k_9 or k_{10}, and k_{dc} can be rewritten as $k_7k_9/(k_7 + k_9)$, and a series of KIE measurements will enable a distinction between the two remaining possible rate-determining steps for V: deglycosylation of the sialosyl-enzyme intermediate (k_7) and a conformational change of the initial enzyme product complex (k_9).

Measurement of KIEs on V can only be made by a direct comparison of individually measured rates of unlabeled and labeled substrates at saturating levels.[24,25] As a consequence, such measurements are prone to greater systematic errors than is the case for competitive KIE measurements made on V/K

dx.doi.org/10.1021/ja109199p | *J. Am. Chem. Soc.* 2011, 133, 2989–2997

Scheme 4. Proposed Catalytic Cycle for Sialidase-Catalyzed Hydrolysis Reactions

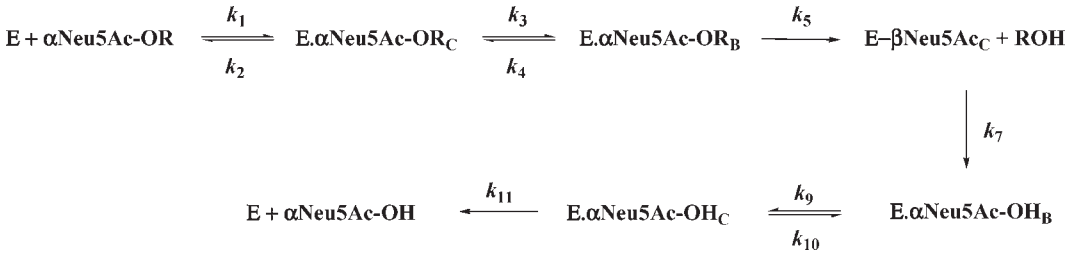

(including varying substrate and enzyme concentrations, changing temperature, and the purity of both isotopic substrates). Despite these innate problems that render the measurement of KIEs on V more difficult, precise and reliable methods have emerged. For example, computer-controlled continuous-flow methods have been reported for the measurement of carbon-13 KIEs (^{13}V)[26,27] for formate dehydrogenase[28] and dialkylglycine decarboxylase.[29]

Ideally, KIEs should be measured on natural substrates; however, such accurate kinetic parameter measurements for sialidases require the use of auxiliary enzymes.[19,30,31] In a recent report, Indurugalla et al. showed that accurate sialidase kinetic parameters could be obtained from α-2,3- and 2,6-sialyl-galactoside linkages, where a chromophore is released in the presence of an *exo*-β-galactosidase.[19] The conditions that are necessary for accurate coupled assays are: (i) the reaction of interest is irreversible and zero-order with respect to the substrate; and (ii) the coupled reaction is irreversible and first-order with respect to the intermediate generated by the primary enzyme.[32] To satisfy these requirements, high substrate concentrations ($\sim 7 \times K_m$) are used and maintained throughout the assay by acquiring data only during the initial 5% of substrate hydrolysis, thus ensuring that the reaction rate is unchanged during the experiment. Also, the use of high concentrations of coupling enzyme (β-galactosidase) ensures that the concentration of the intermediate formed is maintained well below its K_m value for this auxiliary enzyme, and thus ensuring that the reaction is first-order with respect to the intermediate β-galactoside product formed during the sialidase-catalyzed reaction. In the current study, hydrolysis of Neu5Acα2,6GalβFMU (**1**) releases GalβFMU, which in the presence of excess β-galactosidase is rapidly hydrolyzed to liberate the fluorescent aglycone, 8-fluoro-4-methylumbelliferone (FMU), for detection (Scheme 3). Of note, FMU was chosen for this study, rather than the previously used 4-methylumbelliferone leaving group (4-MU),[19] because of its lower pK_a value (6.4 vs 7.8 for 4-MU),[33] and thus at the assay pH, a greater fraction of the liberated phenol is present as its highly fluorescent anion.

Oxygen-18 KIEs. In principle, the measured endocyclic and exocyclic ^{18}O-KIEs for pyranoside and furanoside hydrolysis reactions are complementary.[34,35] That is, the expectation is that one ^{18}O-KIE will be normal ($^{18}k > 1$, C−O bond being broken) and the other will be inverse ($^{18}k < 1$, oxygen atom stabilizing charge development in the nascent oxacarbenium ion).[34,36] The leaving group ^{18}O-KIE for the hydrolysis of **1d** ($^{18}V = 1.003 \pm 0.005$) supports the previous Brønsted analysis[6] that cleavage of the aglycone is not rate-determining. In contrast, the complementary endocyclic oxygen atom is associated with a notably inverse

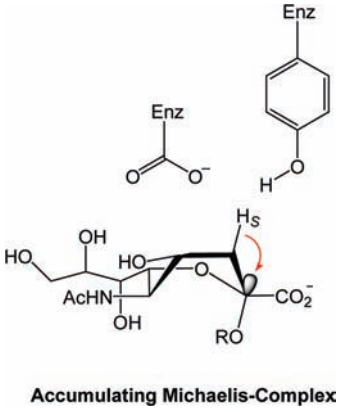

Figure 3. Postulated conformation of the natural substrate analogue in the accumulating Michaelis complex where pro-S σ(C−H) → σ*(C−O) hyperconjugation is maximized.

KIE (**1b**; $^{18}V = 0.986 \pm 0.003$), a result that is consistent with significant charge delocalization occurring onto the pyranosyl oxygen at the deglycosylation transition state (k_7, Scheme 4).

***β*-Secondary Deuterium KIEs.** Generally, solvolysis reactions of carbohydrate derivatives exhibit secondary deuterium KIEs that are normal ($^Dk > 1$), and these effects result from a hyperconjugative weakening of the C−H/D bond by overlap with the nascent ρ-orbital at the anomeric center.[34,37,38] As hyperconjugation is an angular-dependent phenomenon, the magnitude of β-SDKIEs has been used to evaluate transition state (TS) geometry for the glycosylation step (k_S, Scheme 4) for various sialidase-catalyzed reactions.[17,18]

The magnitudes of the two diastereomeric β-secondary deuterium KIEs are markedly different (Table 1) with the 3*S*-isotopomer displaying a large inverse KIE (**1f**; $^DV_S = 0.891$), while the other diastereomer gives rise to a small normal effect (**1e**; $^DV_R = 1.029$). Of note, the C3-dideutero β-SDKIE ($^DV_{R,S} = 0.890 \pm 0.006$) is, within experimental error, the product of the individual axial and equatorial β-SDKIEs. Also, when the substrate concentrations for both unlabeled and dideutero isotopomers were doubled (to approximately $14 \times K_m$), the measured 3-$^2H_2$ KIE was unaltered ($^DV_{R,S} = 0.881 \pm 0.009$; $n = 3$).

The interpretation of the large inverse secondary deuterium KIE for the hydrolysis of **1f** on V is simplified because the magnitude of this KIE ($^DV_S = 0.891$) is outside that normally associated with either steric or inductive effects.[25,39] Thus, the KIE for the 3*S*-isotopomer requires that the rate-limiting step involves a marked strengthening of this C−H/D bond at the TS relative to the ground state. A rationale that requires the accumulating Michaelis complex (reactant state), under the

dx.doi.org/10.1021/ja109199p | J. Am. Chem. Soc. 2011, 133, 2989–2997

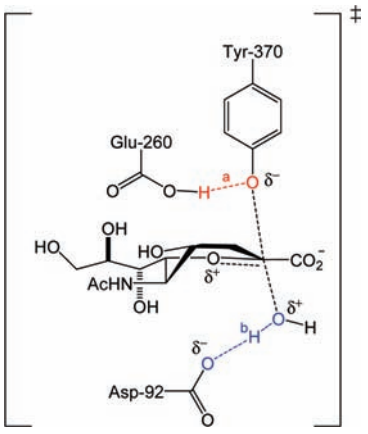

Figure 4. Possible transition state structure for deglycosylation of the β-sialosyl-enzyme intermediate formed during the *M. viridifaciens* sialidase-catalyzed reactions.

conditions of substrate saturation, adopts a conformation in which only one of the two C−H/D bonds is manifestly weakened by a hyperconjugative interaction and that this effect either disappears or considerable weakens at the transition state (Figure 3). That is, hyperconjugative weakening of the equatorial σ(C−H/D) bond into the σ^*(C−O) orbital of the aglycone moiety is the most likely cause for the reduction in the ground-state force constant of this C−H/D bond (Figure 3). Furthermore, there must be little hyperconjugation from the *pro-S* C−H bond into the nascent ρ-orbital at the deglycosylation TS.

A current popular mechanistic rationale for glycosidase-catalyzed reactions, based mainly on X-ray diffraction studies of modified glycosidase:substrate complexes, fluorinated glycosyl-enzyme intermediates, and presumed transition state analogues,[40] is based on the idea that the pyranosyl ring conformation at the TS is close to that of a glycopyranosylium ion (C5, O5, C1, and C2 are coplanar),[41] which in the case of sialidases is proposed to be a $^5H_4$ half-chair (numbering adjusted from ref 40 to match that for sialic acid).[40] Moreover, the postulated reaction coordinate for glycosylation in sialidase-catalysis involves the substrate adopting a $^4S_2$ skew boat in the Michaelis complex and that this converts into a $^2C_5$ chair conformation during formation of the tyrosinyl-bound intermediate.[11]

Of note, the limiting inverse KIE value should occur in cases where the hyperconjugative weakening, which varies as a function of $\cos^2\theta$, is maximal (180° dihedral angle) in the ground state and absent in the TS (90° dihedral angle to the nascent ρ-orbital at the anomeric center). In the context of the inverse KIE ($^DV_S = 0.891$) reported herein, the magnitude of this value is consistent with an accumulating Michaelis complex in which the substrate is positioned in a $^6S_2$ skew-boat conformation (Figure 3) in which maximal hyperconjugative weakening is possible as the dihedral angle between the *pro-S* σ(C−H) bond and the σ^*(C−O) orbital is 180° ($\cos^2\theta = 1$). A conformational change of this $^6S_2$ skew-boat Michaelis complex into a $^4S_2$ conformation, via the $B_{2,S}$, reduces the dihedral angle to around 150° and the interaction by 25% ($\cos^2\theta = 0.75$). Formation of the tyrosinyl-bound intermediate moves the *pro-S* σ(C−H) bond to a dihedral angle of about 60° to the σ^*(C−O) orbital of the anomeric carbon to tyrosine oxygen bond ($^2C_5$ chair conformation; $\cos^2\theta = 0.25$).

Breakdown of the enzyme-bound intermediate (k_7, Scheme 4, Figure 4) involves the anomeric carbon undergoing an oxygen to oxygen electrophilic migration from the enzymatic tyrosine residue to an acceptor water molecule. During this migration, the dihedral angle between the *pro-S* σ(C−H) bond and the nascent ρ orbital at the anomeric center increases from 60° and, based on the inverse secondary deuterium KIE, is likely between 75−105° at the deglycosylation TS ($\cos^2\theta < 0.07$).

The other measured secondary deuterium KIE (**1e**; ^DV_R = 1.029, Table 1) is compatible with a small hyperconjugative interaction at the deglycosylation TS, a result that is consistent with the reported ^Dk values in solution where the *pro-R* value ($^Dk_R = 1.073$) is significantly larger than the corresponding *pro-S* value ($^Dk_S = 1.000$) for the spontaneous hydrolysis of 4-nitrophenyl α-D-sialoside.[21]

Carbon-13 KIEs. The anomeric ^{13}C KIE for the *M. viridifaciens* sialidase-catalyzed hydrolysis of **1a**, $^{13}V = 1.021 \pm 0.006$, is only consistent, when taken with the measured ^{18}V KIEs (Table 1) and the reported β_{lg} value of 0.02 ± 0.03,[6] with the rate-determining step being deglycosylation (k_7, Scheme 4, Figure 4). The measured secondary ^{13}C KIE on carbon 3 (**1c**; $^{13}V = 1.001 \pm 0.008$, Table 1) is equal to one, within experimental error, and this measurement functions as an internal control because it was viewed that ^{13}C-labeling at this position would likely not give rise to a significant KIE.

Typical S_N2 (A_ND_N) reactions of glycosides in solution exhibit ^{13}k values in the range of 1.03−1.08,[37] while carbohydrate hydrolysis reactions that proceed via nonequilibrated short-lived glycopyranosylium ions ($D_N^*A_N$) exhibit ^{13}k values around 1.01.[34,38] Thus, the magnitude of the anomeric ^{13}C KIE ($^{13}V = 1.021 \pm 0.006$) does not allow an unambiguous distinction to be made between the separate mechanistic possibilities. Even so, it is clear that *M. viridifaciens* sialidase-catalyzed deglycosylation involves an "exploded" late transition state[39−41] with significant cleavage of the tyrosinyl-sialoside C−O bond and delocalization of positive charge from the anomeric center occurring via a $n_p(O) \rightarrow \rho(C)$ interaction (**1b**, $^{18}V = 0.986$). The main uncertainty is whether the water nucleophile has started its attack on the anomeric center; indeed the measured anomeric ^{13}C KIE in this study, which is equivalent to a ^{14}C value of around 1.04,[25] is bracketed by two reported ^{14}C KIE measurements of 1.034[42] and 1.041 in which the calculated transition state bond lengths are (i) anomeric carbon−leaving group (C−N in these cases) of 2.65 and 2.80 Å; and (ii) anomeric carbon−oxygen nucleophile of 2.46 and 2.30 Å, respectively. In addition, other calculations have suggested that, for 2-deoxyribosyl reactants, the lower limit for an anomeric ^{13}C-KIE in an A_ND_N mechanism is 1.013−1.040, which encompasses the measured value of 1.021.[43,44] Therefore, it can be concluded that at the transition state for deglycosylation the covalent bond between the anomeric carbon and the enzymatic tyrosine residue is largely broken, while bond formation to the water nucleophile has either not yet begun or just started.

Solvent Deuterium KIE and Proton Inventory. The measured solvent deuterium KIE for the *M. viridifaciens* sialidase-catalyzed hydrolysis of **1** ($^{D_2O}V = 1.585 \pm 0.004$) and the associated linear proton inventory (Figure 4) are consistent with a single proton "in flight" at the transition state. The two plausible proton transfers are shown in Figure 4: (a) general acid-catalyzed protonation of the tyrosine leaving group by Glu260; and (b) general base-assisted nucleophilic attack of water by Asp92.

It can be concluded that the deglycosylation reaction involves general-acid catalysis of tyrosine departure (Figure 4a) as the anomeric carbon KIE is consistent with an exploded, S_N1-like, transition state. That is, without catalysis by Glu-260, the enzymatic tyrosine residue would be required to depart as an

anion with the TS resembling an intimate ion pair, a high energy situation that is ameliorated by general acid catalysis during the rate-limiting cleavage of the sialosyl-tyrosine C−O bond. In contrast, as little or no bond formation is occurring to the nucleophilic water molecule at the TS, the requirement for catalysis by Asp-92 (Figure 4b) is anticipated to be negligible.

Mechanistic Summary. The sialidase from *Micromonospora viridifaciens* operates via a double inversion mechanism in which the accumulating Michaelis complex positions the substrate in a $^6S_2$ skew boat conformation, although, at the present time, it is not certain whether the initial binding event occurs simultaneously with, or prior to, the requisite enzyme-mediated conformational change. However, given that the *M. viridifaciens* sialidase is a remarkable proficient enzyme ($k_{cat}/K_m > 10^7$ M^{-1} s^{-1} with activated substrates),[14] this conformational change is rapid. Next, catalysis occurs via two sequential acetal C−O bond cleavage reactions that occur via an enzyme-bound tyrosinyl β-sialoside intermediate. It is likely that the glycosylation TS is similar to the exploded, S_N1-like, TS noted above for the deglycosylation reaction step. Finally, the product sialic acid dissociates from the enzyme active site.

The possibility that the glycosylation reaction (k_5, Scheme 4) involves formation of an oxacarbenium ion intermediate that reacts directly with water rather than tyrosine-370 deserves comment. For retaining glycosidases, any enzyme-bound intermediate must have a lifetime long enough to allow the aglycone (leaving group) to diffuse from the active site, for a water nucleophile to replace it, otherwise starting material will be regenerated. If the sialidase-bound intermediate is an oxacarbenium ion, rather than an enzymatic tyrosine adduct, then the complex rate constant for dissociation of the carbohydrate leaving group, diffusional association of water, and water attack must be faster than nucleophilic capture of the cation by the proximal tyrosine residue. This possibility seems remote given that Ghanem et al. have estimated the lifetime of an enzyme-bound ribosyl oxacarbenium ion to be less than 50 ps,[45] a lifetime that is too short to allow diffusional separation of the leaving group prior to reaction of the cation.[46]

CONCLUSIONS

A panel of seven isotopically substituted Neu5Acα2,6GalβFMU natural substrate analogues has been used to determine that the rate-limiting step for turnover by the *M. viridifaciens* sialidase is deglycosylation of the β-sialosyl-enzyme intermediate. Furthermore, on the basis of the observed KIEs, it is proposed that the accumulating Michaelis complex places the sialosyl ring in a $^6S_2$ skew boat conformation. The measured KIEs are also consistent with the rate-determining deglycosylation reaction occurring via an exploded transition state in which synchronous charge delocalization is occurring onto the ring oxygen atom. Finally, the proton inventory and the magnitude of the solvent KIE are consistent with general acid-catalyzed protonation of the departing tyrosine residue rather than general base-assisted attack of the nucleophilic water.

ASSOCIATED CONTENT

Supporting Information. Procedures for the syntheses of 8-fluoro-4-methylumbelliferone (FMU) and of 8-fluoro-4-methylumbelliferyl β-D-galactopyranoside (GalβFMU, **6**), ^{1}H NMR spectra and HR−MS molecular ion data for compounds **1**, **1a**−**1g**, and ^{13}C NMR spectra for compounds **1**, **1a**, and **1c**. This material is available free of charge via the Internet at http://pubs.acs.org.

AUTHOR INFORMATION

Corresponding Author
bennet@sfu.ca

ACKNOWLEDGMENT

We thank the Natural Sciences and Engineering Research Council of Canada for financial support and Dr. M. Gilbert (NRC) for providing the 2,6-sialyltransferase. We also thank three anonymous referees for their many helpful comments concerning this manuscript.

REFERENCES

(1) Miyagi, T.; Kato, K.; Ueno, S.; Wada, T. *Trends Glycosci. Glycotechnol.* **2004**, *16*, 371–381.
(2) Schauer, R. *Trends Biochem. Sci.* **1985**, *10*, 357–360.
(3) Corfield, T. *Glycobiology* **1992**, *2*, 509–521.
(4) Taylor, G. *Curr. Opin. Struct. Biol.* **1996**, *6*, 830–837.
(5) Davies, G.; Sinnott, M. L.; Withers, S. G. In *Comprehensive Biological Catalysis*, 1st ed.; Sinnott, M. L., Ed.; Academic Press: San Diego, CA, 1998; pp 119−209.
(6) Watson, J. N.; Dookhun, V.; Borgford, T. J.; Bennet, A. J. *Biochemistry* **2003**, *42*, 12682–12690.
(7) Watson, J. N.; Newstead, S.; Dookhun, V.; Taylor, G.; Bennet, A. J. *FEBS Lett.* **2004**, *577*, 265–269.
(8) Watson, J. N.; Newstead, S.; Narine, A.; Taylor, G.; Bennet, A. J. *ChemBioChem* **2005**, *6*, 1999–2004.
(9) Newstead, S.; Watson, J. N.; Knoll, T. L.; Bennet, A. J.; Taylor, G. *Biochemistry* **2005**, *44*, 9117–9122.
(10) Watts, A. G.; Damager, I.; Amaya, M. L.; Buschiazzo, A.; Alzari, P.; Frasch, A. C.; Withers, S. G. *J. Am. Chem. Soc.* **2003**, *125*, 7532–7533.
(11) Watts, A. G.; Oppezzo, P.; Withers, S. G.; Alzari, P. M.; Buschiazzo, A. *J. Biol. Chem.* **2006**, *281*, 4149–4155.
(12) Chan, J.; Lewis, A. R.; Gilbert, M.; Karwaski, M. F.; Bennet, A. J. *Nat. Chem. Biol.* **2010**, *6*, 405–407.
(13) Chong, A. K. J.; Pegg, M. S.; Taylor, N. R.; von Itzstein, M. *Eur. J. Biochem.* **1992**, *207*, 335–343.
(14) Narine, A. A.; Watson, J. N.; Bennet, A. J. *Biochemistry* **2006**, *45*, 9319–9326.
(15) Lowry, T. H.; Richardson, K. S. *Mechanism and Theory in Organic Chemistry*, 3rd ed.; Harper & Row: New York, 1987.
(16) Guo, X.; Laver, W. G.; Vimr, E.; Sinnott, M. L. *J. Am. Chem. Soc.* **1994**, *116*, 5572–5578.
(17) Guo, X.; Sinnott, M. L. *Biochem. J.* **1993**, *294*, 653–656.
(18) Sinnott, M. L.; Guo, X. M.; Li, S. C.; Li, Y. T. *J. Am. Chem. Soc.* **1993**, *115*, 3334–3335.
(19) Indurugalla, D.; Watson, J. N.; Bennet, A. J. *Org. Biomol. Chem.* **2006**, *4*, 4453–4459.
(20) Karwaski, M. F.; Wakarchuk, W. W.; Gilbert, M. *Protein Expression Purif.* **2002**, *25*, 237–240.
(21) Ashwell, M.; Guo, X.; Sinnott, M. L. *J. Am. Chem. Soc.* **1992**, *114*, 10158–10166.
(22) Indurugalla, D.; Bennet, A. J. *Can. J. Chem.* **2008**, *86*, 1005–1009.
(23) Bergson, G.; Matsson, O.; Sjoberg, S. *Chem. Scr.* **1977**, *11*, 25–31.
(24) Cook, P. F.; Cleland, W. W. *Enzyme Kinetics and Mechanism*; Garland Science: London; New York, 2007.
(25) Melander, L. C. S.; Saunders, W. H. J. *Reaction Rates of Isotopic Molecules*; Wiley: New York, 1980.
(26) Cook, P. F.; Cleland, W. W. *Biochemistry* **1981**, *20*, 1790–1796.

(27) Northrop, D. B. *Biochemistry* **1975**, *14*, 2644–2651.
(28) Xue, H.; Wu, X. W.; Huskey, W. P. *J. Am. Chem. Soc.* **1996**, *118*, 5804–5805.
(29) Zhou, X.; Toney, M. D. *J. Am. Chem. Soc.* **1998**, *120*, 13282–13283.
(30) Alon, R.; Bayer, E. A.; Wilchek, M. *J. Biochem. Biophys. Methods* **1991**, *22*, 23–33.
(31) Ziegler, D. W.; Hutchinson, H. D. *Appl. Microbiol.* **1972**, *23*, 1060–1066.
(32) Segel, I. H. *Enzyme Kinetics: Behavior and Analysis of Rapid Equilibrium and Steady State Enzyme Systems*; Wiley: New York, 1975.
(33) Sun, W. C.; Gee, K. R.; Haugland, R. P. *Bioorg. Med. Chem. Lett.* **1998**, *8*, 3107–3110.
(34) Bennet, A. J.; Sinnott, M. L. *J. Am. Chem. Soc.* **1986**, *108*, 7287–7294.
(35) Bennet, A. J.; Sinnott, M. L.; Wijesundera, W. S. S. *J. Chem. Soc., Perkin Trans. 2* **1985**, 1233–1236.
(36) Bennet, A. J.; Davis, A. J.; Hosie, L.; Sinnott, M. L. *J. Chem. Soc., Perkin Trans. 2* **1987**, 581–584.
(37) Kresge, A. J.; Weeks, D. P. *J. Am. Chem. Soc.* **1984**, *106*, 7140–7143.
(38) Tanaka, Y.; Tao, W.; Blanchard, J. S.; Hehre, E. J. *J. Biol. Chem.* **1994**, *269*, 32306–32312.
(39) Buncel, E.; Lee, C. C. *Secondary and Solvent Isotope Effects*; Elsevier: Amsterdam; New York, 1987.
(40) Vocadlo, D. J.; Davies, G. J. *Curr. Opin. Chem. Biol.* **2008**, *12*, 539–555.
(41) Sinnott, M. *Carbohydrate Chemistry and Biochemistry: Structure and Mechanism*; RSC Publishing: Cambridge, 2007.
(42) Berti, P. J.; Blanke, S. R.; Schramm, V. L. *J. Am. Chem. Soc.* **1997**, *119*, 12079–12088.
(43) Berti, P. J.; Tanaka, K. S. E. *Adv. Phys. Org. Chem.* **2002**, *37*, 239–314.
(44) Chen, X.-Y.; Berti, P. J.; Schramm, V. L. *J. Am. Chem. Soc.* **2000**, *122*, 6527–6534.
(45) Ghanem, M.; Murkin, A. S.; Schramm, V. L. *Chem. Biol.* **2009**, *16*, 971–979.
(46) Richard, J. P.; Jencks, W. P. *J. Am. Chem. Soc.* **1984**, *106*, 1373–1383.
(47) Taylor, J. R. *An Introduction to Error Analysis: The Study of Uncertainties in Physical Measurements*; University Science Books: Mill Valley, CA, 1982.